molecular pharmaceutics

From Physical Mixtures to Co-Crystals: How the Coformers Can Modify Solubility and Biological Activity of Carbamazepine

Alessandro Dalpiaz,[†] Valeria Ferretti,*,[†] Valerio Bertolasi,[†] Barbara Pavan,*,[‡] Antonio Monari,[§,∥] and Mariachiara Pastore*,[§,∥]

[†]Department of Chemical and Pharmaceutical Sciences, University of Ferrara, via Fossato di Mortara 17, I-44121 Ferrara, Italy

[‡]Department of Life Sciences and Biotechnology, University of Ferrara, via L. Borsari 46, I-44121 Ferrara, Italy

[§]Laboratoire de Physique et Chimie Théoriques, Université de Lorraine, Boulevard des Aiguillettes, BP 70239 54506 Vandoeuvre-lès-Nancy Cedex, France

[∥]Laboratoire de Physique et Chimie Théoriques, CNRS, Boulevard des Aiguillettes, BP 70239 54506 Vandoeuvre-lès-Nancy Cedex, France

S Supporting Information

ABSTRACT: A combined experimental and computational study on the solubility and biological activity of carbamazepine (CBZ), three co-crystals (COCs), and their parent physical mixtures (MIXs) is carried out to shed light onto the possible modulation of the drug properties. Two of the considered co-crystals, CBZ with vanillic acid (VAN) and CBZ with 4-nitropyridine N-oxide (NPO), are newly synthesized, while the third, CBZ with succinic acid (SUC), is already known. While COC CBZ-VAN and MIX CBZ-NPO did not alter the CBZ dissolution profile, MIX CBZ-SUC and COCs CBZ-SUC and CBZ-NPO inhibit straightaway its solubility. On the other hand, MIX CBZ-VAN induced a remarkable increase of the drug solubility. Analogously, different CBZ permeability values were registered following its dissolution from MIXs and COCs: CBZ and MIXs CBZ-SUC and CBZ-VAN slightly reduce the integrity of intestinal cell monolayers, whereas MIX CBZ-NPO and COCs CBZ-SUC, CBZ-VAN, and CBZ-NPO maintain the monolayer integrity. The molecular aggregates formed in solution were found to be the key to interpret these different behaviors, opening new possibilities in the pharmaceutical utilization and definition of drug co-crystals.

KEYWORDS: co-crystals, carbamazepine, drug permeation, molecular dynamics
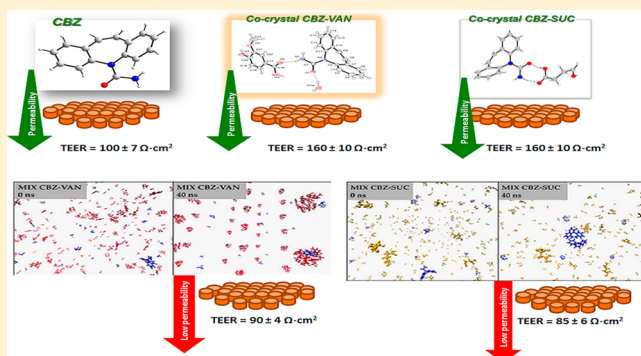
INTRODUCTION

The therapeutic efficiency of drugs is strictly related to their bioavailability, which, in turn, is often linked to their solubility and permeability across biological membranes.[1] However, since poorly soluble molecules constitute a high percentage of approved drugs[2] and several marked drugs do not exhibit adequate permeability properties,[3] the development of improved formulations of existing drugs is one of the most relevant and successful scientific and market-oriented strategies.[2] In this context, the co-crystallization approach appears promising to achieve the crystal engineering of pharmaceutical solids.[4] Generally speaking, a co-crystal can be defined as a crystalline complex of two or more molecules, usually present in a stoichiometric ratio.[5,6] Pharmaceutical co-crystals are obtained by combining a pharmaceutical active ingredient (API) with pharmaceutically acceptable molecules, assembled through intermolecular interactions.[7,8] The latter are generally different from those found in the crystals of the pure components; consequently, these new crystalline forms exhibit specific physical properties, retaining at the same time the unaltered chemical structure of the APIs. Indeed, it is currently believed that the co-crystallization strategy should not induce changes in the native APIs' pharmacological profile.[9−12] Pharmaceutical co-crystals can show higher solubility and dissolution rate compared to parent crystalline pure phases,[2] with consequent improvement of the bioavailability of APIs[13] even if the latter is not a systematic phenomenon.[14] Moreover, preliminary studies suggest that co-crystals can offer the opportunity to simultaneously improve both the solubility and the permeability of APIs, without changing their molecular structure.[9,15,16] Very recently a co-crystal salt of norfloxacin and sulfathiazole was reported to enhance inhibition of bacterial and fungal strains as a result of joint solubility and diffusion increase.[17] As such the modulation of co-crystal based formulations has emerged as one of the most exciting areas

A

of novel pharmaceuticals; indeed, the past decade has registered a significant increase in the number of patents on pharmaceutical co-crystals, which are characterized by the required features of novelty, nonobviousness/inventiveness, and utility.[1] The regulatory status regarding the use of co-crystals in pharmaceutical products appears, however, still unsettled, and, in particular, the issue whether the co-crystal should be defined as a physical mixture or as a new chemical entity requiring full safety and toxicology testing has not been properly addressed, yet.[18,19] Both the United States Food and Drug Administration (US FDA) and the European Medicines Agency (EMA) have delivered position documents regarding pharmaceutical co-crystals, but their points of view on this topic are contrasting.[14] With the aim of gaining a deeper knowledge of these aspects, and hence also hopefully assisting policy-making strategies, we have recently compared the properties of indomethacin co-crystals with those of their parent physical mixtures, focusing on the drug permeability across monolayers constituted by human intestinal cells.[6] Our results revealed, for the first time, that the effects of an API dissolved either from the co-crystals or from their parent physical mixtures can have extremely different effects on the integrity of cell monolayers and API permeability, hence evidencing an intriguing phenomenon and the emergence of entirely new biological and chemical properties following co-crystallization. As a consequence, the properties of pharmaceutical co-crystals can be assumed to be, in certain cases, drastically different from those of their parent physical mixtures.[6]

As a further development of this type of investigation, we report here an evaluation of the dissolution properties and the permeation ability across human intestinal cell monolayers of (i) carbamazepine (CBZ), a poorly water-soluble antiepileptic drug;[20] (ii) two new CBZ co-crystals with vanillic acid (VAN) and 4-nitropyridine N-oxide (NPO); and (iii) a previously described CBZ co-crystal with succinic acid (SUCC).[21] All studies are referred to carbamazepine, considered as the active drug. The schematic representation of CBZ and the coformers is shown in Scheme 1.

In particular, the dissolution and the permeation across NCM460 cell monolayers (employed as an *in vitro* model of human intestinal epithelial barrier)[6] of CBZ, its co-crystals, and their parent mixtures have been investigated. Moreover, we performed quantum mechanical (DFT) and classical molecular dynamics (MD) simulations, since integrated experimental and theoretical investigation could represent an important step toward the detailed understanding, at a molecular level, of the different solubility and biological activity of co-crystals and the physical mixtures of its components, opening new perspectives in their pharmaceutical utilization as well as the co-crystals' rational design.

This strategy has been purposely chosen to (i) quantify the strength and identify the topology of the main pair (CBZ-CBZ and CBZ-coformer) interactions in solution in comparison to the ones found in the crystal and co-crystal structures and (ii) mimic in an explicit water environment the behavior of different concentrations of CBZ and coformers, possibly experienced in the dissolution from co-crystals and from the physical mixtures of the two components.

■ MATERIALS AND METHODS

Materials and Reagents. Carbamazepine (CBZ), 4-nitropyridine N-oxide (NPO), succinic acid (SUCC), vanillic acid (VAN), 2-aminopyrimidine (2-ampyr), 2,4-diamino-6-phenyl-1,3,5-triazine (triaz), and picric acid (Pic) were obtained from Sigma-Aldrich (Milan, Italy). Methanol, ethanol, isoamyl acetate, isoamyl alcohol, toluene, and water were of high performance liquid chromatography (HPLC) grade from Sigma-Aldrich. NCM-460 cells were kindly provided by Dr. Antonio Strillacci, University of Bologna, Italy.

Synthesis of Adducts. Five carbamazepine co-crystals were synthesized and characterized by X-ray crystallography. CBZ-VAN: carbamazepine, vanillic acid monohydrate 1:1:1. CBZ-NPO: carbamazepine and 4-nitropyridine N-oxide 1:1. CBZ-Pic: carbamazepine and picric acid 1:1 (ionic). CBZ-2ampyr: carbamazepine and 2-aminopyrimidine 1:1. CBZ-triaz: carbamazepine and 2,4-diamino-6-phenyl-1,3,5-triazine 1:1. The last three adducts were not used in the present work for their scarce reproducibility and/or for the high coformer toxicity; details of the related crystallographic analysis are reported in Table S1. Co-crystal CBZ-SUCC[21] has been obtained by slow evaporation of a biphasic solution made of toluene, isoamyl alcohol, and water containing equimolar drug/succinic acid quantity. All other co-crystals have been obtained by dissolution of an equimolar quantity of carbamazepine and co-crystal partners in the minimum quantity of isoamyl acetate/toluene mixture or ethanol and left for slow evaporation at room temperature. Crystals were observed after a few days. The phase and composition of the co-crystals CBZ-NPO, CBZ-SUCC, and CBZ-VAN have been checked by X-ray powder crystallography, comparing the experimental spectra with those calculated from the single-crystal X-ray structures (Figures S4–S6).

X-ray Diffraction. Detailed description of single-crystal data collection and refinement for all the new co-crystals and of powder diffraction spectra for co-crystals CBZ-VAN, CBZ-NPO, and CBZ-SUCC are reported in the Supporting Information. Experimental data for single-crystal diffraction and geometrical and hydrogen bonding parameters are given in Tables S1–S3, respectively.

Crystallographic data for the structural analysis of the five new compounds have been deposited at the Cambridge Crystallographic Data Center, 12 Union Road, Cambridge, CB2 1EZ, U.K., with the deposition numbers CCDC

Scheme 1. Schematic representation of carbamazepine and coformers

Carbamazepine

Vanillic acid

Succinic acid

4-nitropyridine-N-oxyde
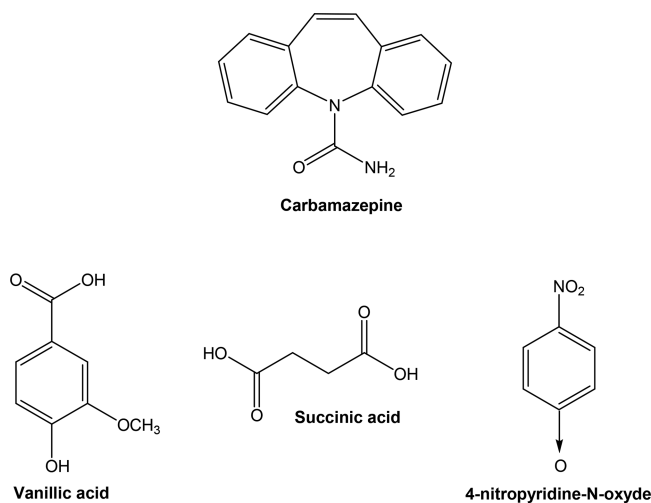
1507263−1507267 for CBZ-NPO, CBZ-ampyr, CBZ-VAN, CBZ-triaz, and CBZ-Pic, respectively.

HPLC Analysis. The quantification of carbamazepine was performed by HPLC, using a modular system (model LC-10 AD VD pump and model SPD-10A VP variable wavelength UV−vis detector; Shimadzu, Kyoto, Japan) and an injection valve with 20 μL sample loop (model 7725; Rheodyne, IDEX, Torrance, CA, USA). Separation was performed at room temperature on a reverse phase column, equipped with a guard column, both packed with Hypersil BDS C-18 material (Alltech Italia Srl BV, Milan, Italy). Data acquisition and processing were accomplished using CLASS-VP Software, version 7.2.1 (Shimadzu Italia, Milan, Italy). The detector was set at 286 nm. The mobile phase consisted of a methanol−water mixture (50:50 v/v). The flow rate was 1 mL/min. The retention time for carbamazepine was 5.2 min; precision and calibration data are reported in the Supporting Information.

Dissolution Studies. The samples were micronized and sieved using stainless steel standard-mesh sieves (mesh size 106 μm). In each experiment, the solid powders were added to 12 mL of PBS 10 mM and incubated at 37 °C under gentle shaking (100 rpm) in a water bath. The amounts of sieved samples added to the buffer solution were 38.0 mg of carbamazepine; 67.9 mg of co-crystal CBZ-VAN; 55.4 mg of co-crystal CBZ-SUCC; 60.5 mg of co-crystal CBZ-NPO; 38 mg of carbamazepine mixed with 27.7 mg of vanillic acid, 17.4 mg of succinic acid, or 22.5 mg of 4-nitropyridine N-oxide for the parent physical mixtures CBZ-VAN, CBZ-SUCC, or CBZ-NPO, respectively. Aliquots (200 μL) were withdrawn from the resulting slurry at fixed time intervals and filtered through regenerated cellulose filters (0.45 μm). The filtered samples were diluted 1:10 in water, and then 10 μL was injected into the HPLC system in order to quantify the carbamazepine concentrations.

Dissolution experiments were conducted also in phosphate buffer 200 mM (pH = 7.4) at 37 °C with the same procedure. The obtained values were the mean of three independent experiments.

Cell Culture and Differentiation of NCM460 Cells to Polarized Monolayers. The NCM460 cell line was grown and differentiated to cell monolayers in 12-well Millicell inserts (Millipore, Milan, Italy) essentially as previously described[6] and reported in the Supporting Information.

Permeation Studies across Cell Monolayers. Inserts were washed twice with prewarmed PBS buffer in the apical (A, 400 μL) and basolateral (B, 2 mL) compartments; PBS buffer containing 5 mM glucose at 37 °C was then added to the apical compartment. The sieved powders were added to the apical compartments in the following amounts: 1.3 mg of carbamazepine; 2.3 mg of co-crystal CBZ-VAN; 1.8 mg of co-crystal CBZ-SUCC; 2.0 mg of co-crystal CBZ-NPO; 1.3 mg of carbamazepine mixed with 0.90 mg of vanillic acid, or 0.50 mg of succinic acid, or 0.75 mg of 4-nitropyridine N-oxide for mixtures MIX CBZ-VAN, CBZ-SUCC, or CBZ-NPO, respectively. During permeation experiments, Millicell inserts loaded with the powders were continuously swirled on an orbital shaker (100 rpm; model 711/CT, ASAL, Cernusco, Milan, Italy) at 37 °C. At programmed time points the inserts were removed and transferred into the subsequent wells containing fresh PBS; then basolateral PBS was harvested, filtered through regenerated cellulose filters (0.45 μm), and injected (10 μL) into the HPLC system for carbamazepine detection. At the end of incubation the apical slurries were

withdrawn, filtered, and injected into the HPLC system (10 μL) after 1:10 dilution. After the withdrawal, 400 μL of PBS was inserted in the apical compartments and TEER measurements were performed. Permeation experiments were also conducted using cell-free inserts in the same conditions. The values obtained were the mean of three independent experiments. Apparent permeability coefficients (P_{app}) of carbamazepine were calculated according to eq 1:[22−24]

$$P_{app} = \frac{\frac{dc}{dt}V_r}{S_A C}$$

(1)

where P_{app} is the apparent permeability coefficient in cm/min; dc/dt is the flux of drug across the filters, calculated as the linearly regressed slope through linear data; V_r is the volume in the receiving compartment (basolateral = 2 mL); S_A is the diffusion area (1.13 cm^2); C is the compound concentration in the donor chamber (apical) detected at 60 min and chosen as approximate apical concentration. Statistical analysis about permeation studies is described in the Supporting Information.

Computational Details. The binding energies of CBZ-CBZ and CBZ-VAN, CBZ-SUC, and CBZ-NPO dimers interacting by hydrogen bond (HB) and/or π-stacking (S) were calculated by the M06-2X[25] functional in combination with a 6-31G* basis set and an implicit description of the water medium (C-PCM)[26] as implemented in the Gaussian09 package.[27] The dimer structures were optimized in water solution, and the interaction energy was obtained as difference between the energy of the complex and those of the optimized monomers. We also performed MD simulations of binary systems composed of different concentrations of drug and coformers, representative of the dissolved co-crystals and physical mixtures using the generalized Amber force field (GAFF);[28] electrostatic point charges were parametrized using the RESP protocol, and fitting the quantum chemical potential calculated at the HH/6-31G* level of theory. Drugs and coformers were embedded in a periodic cubic water box of ca. 100 × 100 × 100 Å^3 filled with water molecules in order to reproduce bulk conditions. For mimicking the early stage of dissolution from the COC we started the MD runs with a 4:4 cluster (CBZ:VAN, CBZ:SUC, and CBZ:NPO) extracted from the co-crystal structure in such a way as to work at low concentration and with the same ratio of drug−coformer. A reference MD simulation of 4 molecules of CBZ in the same water box was also carried out. The CBZ-VAN, CBZ-SUC, and CBZ-NPO MIX solutions were instead simulated by randomly distributing, by using the PACKMOL package,[29] in the water box 2 molecules of CBZ and 20, 32, and 32 molecules of VAN, SUC, and NPO, respectively. These ratios were determined by considering the relative saturation concentrations of the drug and coformers: 0.18 mg/mL, 1.33 mg/mL, 1.45 mg/mL, and 1.88 mg/mL for CBZ, VAN, SUC, and NPO, respectively. The full system was preliminarily optimized using the steepest descent algorithm to remove bad contacts; subsequently a thermalization procedure was performed in the NVT ensemble, gradually bringing the temperature to 300 K; this step was followed by equilibration in the NPT ensemble ensuring the density of the ensemble to be close to 1 g/cm^3. Once equilibrated, the system underwent 40 ns of production run in the NPT ensemble. Radial distribution functions ($g(r)$) were obtained between the CBZ and the coformer (see Figure S9 for a proper definition of the involved atoms) in the range 10−40 ns of the trajectories. Even though we are aware that the
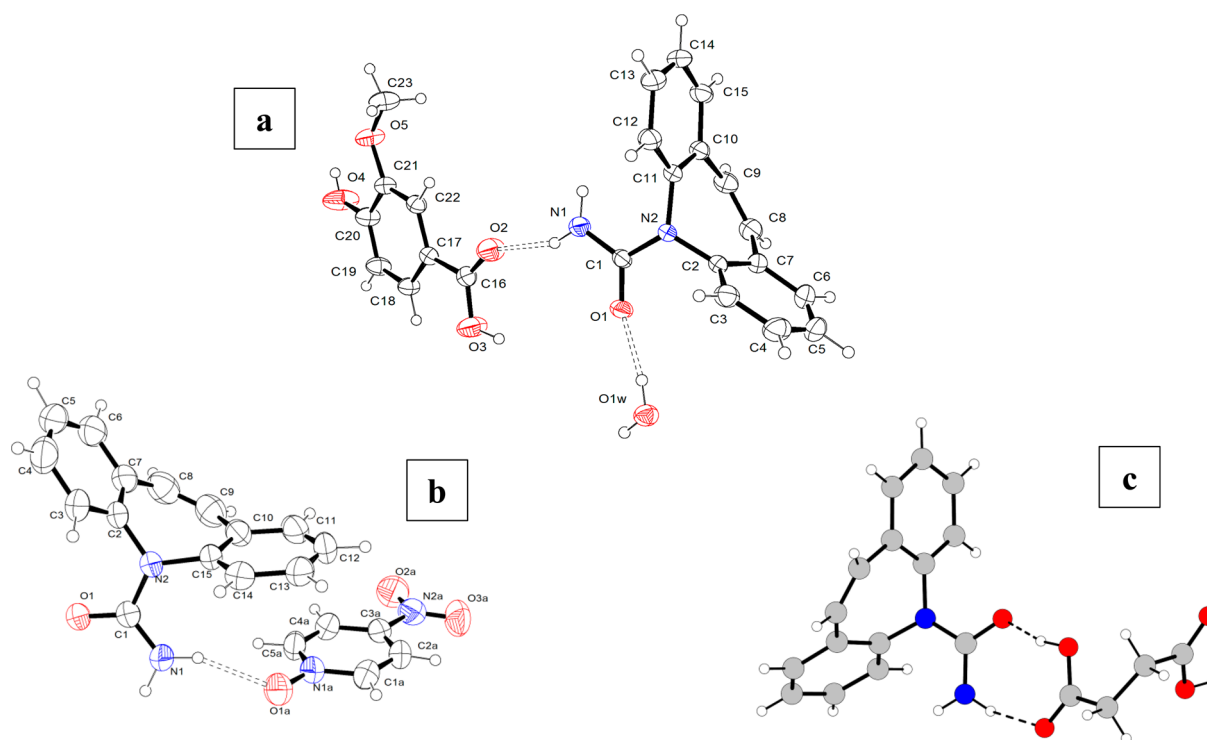
Figure 1. (a) ORTEPIII[32] view and atom numbering scheme for CBZ-VAN. (b) ORTEPIII view and atom numbering scheme for CBZ-NPO. (c) Carbamazepine-succinic acid co-crystal CBZ-SUCC (from ref [20]). Thermal ellipsoids are drawn at the 40% probability level. Hydrogen bonds are drawn as dashed lines.
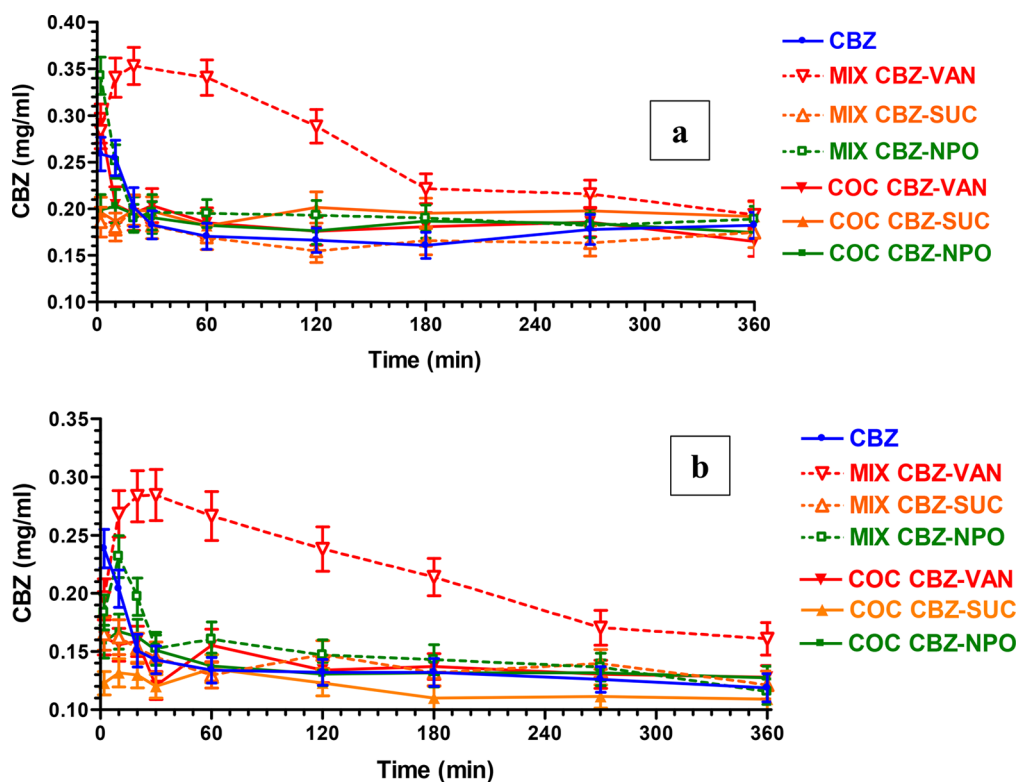
Figure 2. Solubility and dissolution profiles in PBS 10 mM (a) and phosphate buffer 200 mM (b) at 37 °C for carbamazepine (CBZ) as free drug, or co-crystallized, or mixed in the parent mixtures. Data are reported as the mean ± SD of three independent experiments.

number of involved molecules is too low to allow the convergence toward macroscopic thermodynamics properties, this strategy is adapted to obtain the distribution of the distances between the solute and all the possible molecules averaged over a consistent segment of the trajectory. All simulations and setups have been performed using the

Amber16[30] code and its CUDA extension, while analysis and visualization have been performed using the VMD code.[31]

RESULTS AND DISCUSSION

Structure Description. Five new co-crystals containing carbamazepine have been synthesized and characterized by X-ray crystallography: CBZ-VAN (carbamazepine and vanillic acid monohydrate 1:1:1); CBZ-NPO (carbamazepine and 4-nitropyridine N-oxide) 1:1; CBZ-Pic (carbamazepine and picric acid 1:1, salt); CBZ-2ampyr (carbamazepine and 2-amino-pyrimidine 1:1); and CBZ-triaz (carbamazepine and 2,4-diamino-6-phenyl-1,3,5-triazine 1:1). However, in spite of many attempts, it was possible to synthesize in appreciable quantity only CBZ-VAN and CBZ-NPO, besides the previously reported carbamazepine-succinic acid co-crystal (CBZ-SUCC).[20] The crystal structure details of CBZ-Pic, CBZ-2ampyr and CBZ-triaz are reported in the Supporting Information.

The X-ray structures of the three adducts used in the present study are shown in Figure 1; the main hydrogen bonding interactions between the molecules are drawn as dashed lines. In CBZ-VAN, the two coformers are directly linked through a N−H···O interaction involving the amidic group of the drug and the carboxylic group of the acid (see Table S3). Each co-crystallized water molecule acts both as a H-bond donor (toward the O1 atom of two adjacent carbamazepine moieties) and H-bond acceptor (from O3 and O4 of two vanillic acid molecules), in such a way as to bridge four different molecules (Figure 1a). C−H···π and π···π interactions appear to be quite important, as all the aromatic rings of the two molecules are involved (Table S3). Although the packing architecture is mainly determined by these interactions, some weaker C−H···O hydrogen bonds also contribute to the crystal stability. Conversely, in CBZ-NPO the carbamazepine molecules are coupled in dimeric units by N1−H···O1 hydrogen bonds, as found in the crystal lattice of the pure carbamazepine polymorph III crystal.[33] In turn, each dimer is linked on both sides to two nitropyridine coformers through N1−H···O1A hydrogen bonds involving the carbamazepine amidic group, and the N-oxide group of the coformer molecule (Figure 1b). Besides these classical hydrogen bonds, each NPO molecule forms π···π interactions with the C10−C15 aromatic ring of two stacked CBZ molecules (Table S3). More details about the crystals structures and the packing arrangements can be found in the Supporting Information.

Dissolution Studies. In order to check if co-crystallization can affect the solubility of pure carbamazepine, dissolution studies have been performed by the HPLC method (vide infra). Figure 2a reports a comparison between the dissolution profiles in PBS 10 mM (pH 7.4) at 37 °C of carbamazepine, as free drug, co-crystallized, or mixed in the parent mixtures. The concentration of free CBZ was 0.26 ± 0.02 mg/mL after 2 min of incubation, and then it decreased to a stable value of about 0.18 ± 0.01 mg/mL within 30 min of incubation. Among the four anhydrous polymorphic forms of CBZ, we used the most stable at room temperature, i.e., the anhydrous polymorphic form of CBZ(III) that, in water, is known to convert itself to the dihydrate form (DH), inducing a decrease of CBZ water solubility.[34,35] The dissolution pattern of this drug, reported in Figure 2, perfectly matches the expected trend due to its conversion from the anhydrous polymorph (III) to the dihydrate form. This dissolution profile was not essentially altered by the co-crystallization of carbamazepine with vanillic acid (COC CBZ-VAN) or by its mixing with 4-nitropyridine N-oxide (MIX CBZ-NPO), whereas the co-crystallization with succinic acid (COC CBZ-SUCC) or 4-nitropyridine N-oxide (COC CBZ-NPO) allowed a stable carbamazepine saturation concentration of about 0.18 ± 0.01 mg/mL to be obtained within 2 min of incubation. The same pattern was observed also in the presence of succinic acid, when mixed with the drug (MIX CBZ-SUCC).

On the other hand, the dissolution profile of carbamazepine obtained in the presence of vanillic acid, as physical mixture (MIX CBZ-VAN), was characterized by an increase of concentration from 0.28 ± 0.02 mg/mL to 0.35 ± 0.02 mg/mL in the time range 2−20 min, and then the drug concentration slightly decreased to about 0.18 ± 0.01 mg/mL within 6 h. A qualitatively similar behavior was observed for the CBZ dissolution from a mixture with nicotinamide.[36] The PBS 10 mM was chosen as dissolution medium being employed for the permeation studies across the intestinal cell monolayers (see below). The pH value of this medium sensibly decreased in the presence of succinic and vanillic acids from 7.4 to about 5.

The carbamazepine solubility and dissolution profiles (Figure 2a) did not essentially change when the powders were incubated in phosphate buffer 200 mM, the medium employed in order to obtain pH stability at the 7.4 value. As reported in Figure 2b, the dissolution patterns were close to those obtained by incubation of the powders in 10 mM PBS, indicating that the carbamazepine dissolution is independent of the pH of the incubation medium.

Permeation Studies. Currently, a limited number of studies describe the ability of co-crystals to modulate the permeability of APIs across the skin,[37] or dialysis, silicone, and cellulose nitrate membranes.[9,16,17] Very recently, we have reported on the remarkably different permeation across a monolayer constituted by human intestinal cells of indomethacin dissolved from co-crystals or parent powder.[6] Hence we decided to perform permeation experiments, across human intestinal cell monolayers, also for carbamazepine dissolved from the anhydrous polymorph form (III), from its co-crystals or their parent physical mixtures. As an in vitro model system of a human intestinal barrier, we have chosen the human normal colonic epithelial NCM460 cells, a stabilized, non-transformed cell line, derived from primary cells of the normal human transverse colonic mucosa.[38] As these cells are not of tumor origin nor transfected ones, they retain more closely the physiological characteristics of the normal human colon compared to the pathologically or experimentally transformed cell lines. In this context, it is worth noting that transepithelial electrical resistance (TEER) developed by the NCM460 cells are within the range reported for intact sheets of human colonic mucosa.[39,40] After confluence in "Millicell" systems, the cell layer separated an apical from a basolateral compartment corresponding to the lumen facing domain and the blood-facing side of the monolayer, respectively.[41] This system provided a very useful tool in order to simulate in vitro the permeation of CBZ across the intestinal barrier. It is known that simulated intestinal buffers can induce TEER changes of the monolayers and have inhibitory activity toward efflux transporters expressed on the cell membranes.[42] Therefore, the permeation studies across NCM460 cells, in the absence of other interfering substances, were performed using glucose-enriched PBS as CBZ dissolution medium, i.e., the simplest medium in which to dissolve the API from its powders. In order to simulate an oral
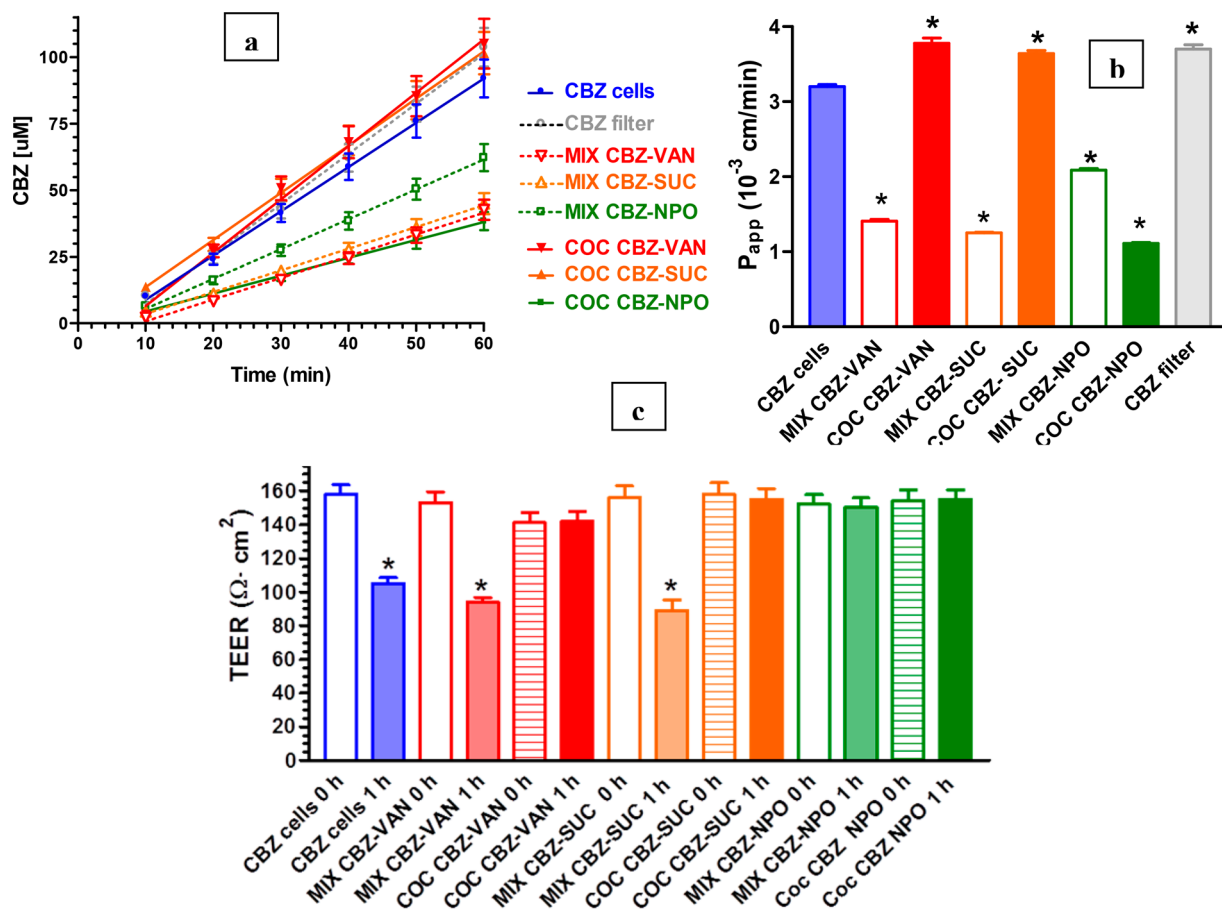
Figure 3. (a) Permeation kinetics of carbamazepine after introduction in the "Millicell" apical compartments of powders constituted by carbamazepine (CBZ), its co-crystals, or the parent mixtures of carbamazepine with co-crystallizing agents. The permeations were analyzed across monolayers obtained by NCM460 cells. Millicell filters alone (filter) or coated by monolayers (cells) were used to analyze the carbamazepine permeation. The cumulative amounts in the basolateral receiving compartments were linear within 60 min ($r \geq 0.998$, $P < 0.001$). The resulting slopes of the linear fits were used for the calculation of permeability coefficients (P_{app}). (b) Permeability coefficients (P_{app}) of carbamazepine. All data related to permeation studies are reported as the mean $\pm$ SD of three independent experiments. *$P < 0.001$ versus CBZ cells. (c) Transepithelial electrical resistance (TEER) values of NCM460 cell monolayers obtained when cell cultures reached the confluence. Parallel sets of "Millicell" well plates with similar TEER values were measured before (0 h) and at the end (1 h) of incubation with carbamazepine, its co-crystals, and parent physical mixtures. The data are reported as the mean $\pm$ SD of three independent experiments. *$P < 0.001$ versus 0 h.

administration, the powders of carbamazepine, its co-crystals, or the parent physical mixtures were introduced in the apical compartment of the "Millicell" systems with the same ratio between solid powders and incubation conditions used for dissolution studies, during the analysis time period for all samples. The cumulative amounts in the basolateral receiving compartments were linear within 60 min ($r \geq 0.998$, $P < 0.001$), indicating constant permeation conditions within this range of time (Figure 3a).

The apparent permeability coefficients (P_{app}) of carbamazepine (Figure 3b) were calculated on the basis of the resulting slopes of the linear fits and the drug concentrations detected in the apical compartments after 1 h of incubation of the powders, chosen as approximate apical concentrations. These latter values were essentially in line with those obtained from dissolution studies of carbamazepine powders in 10 mM PBS (Figure 3a), so their dissolution appeared slightly influenced by the presence of the cells. A comparison of the P_{app} values of carbamazepine (Figure 3b) obtained in the presence ($3.20 \times 10^{-3} \pm 0.05 \times 10^{-3}$ cm/min) or in the absence ($3.71 \times 10^{-3} \pm 0.10 \times 10^{-3}$ cm/min) of NCM460 cell monolayers indicated a lower permeation of the drug in the presence of cells than in

their absence ($P < 0.001$). Even if significant, this difference of P_{app} values was relatively small (0.5×10^{-3} cm/min), indicating a high aptitude of carbamazepine to permeate across the NCM460 cell monolayer. This phenomenon was related to the ability of the drug to decrease the TEER value of the monolayer from 160 $\Omega \cdot cm^2$ (a value indicating its integrity) to about 100 $\Omega \cdot cm^2$ ($P < 0.001$), during its incubation (Figure 3c), hence suggesting the capacity of carbamazepine to open the tight junctions of the NCM460 cells. A similar effect on the TEER values was also observed when carbamazepine was mixed with the vanillic and succinic acids (MIX CBZ-VAN and MIX CBZ-SUCC, Figure 3c), whose presence induced, however, a reliable decrease ($P < 0.001$) of the P_{app} value of the drug from $3.20 \times 10^{-3} \pm 0.05 \times 10^{-3}$ cm/min (CBZ) to $1.41 \times 10^{-3} \pm 0.04 \times 10^{-3}$ cm/min (MIX CBZ-VAN) or $1.25 \times 10^{-3} \pm 0.02 \times 10^{-3}$ cm/min (MIX CBZ-SUCC), as reported in Figure 3b. This P_{app} decrease was not observed when the vanillic or succinic acids were introduced in the "Millicell" systems as co-crystals of carbamazepine; on the contrary, in this case the P_{app} value of the drug increased ($P < 0.001$) from $3.20 \times 10^{-3} \pm 0.05 \times 10^{-3}$ cm/min (CBZ) to $3.78 \times 10^{-3} \pm 0.02 \times 10^{-3}$ cm/min (COC CBZ-VAN) or $3.64 \times 10^{-3} \pm 0.02 \times 10^{-3}$ cm/min (COC

CBZ-SUCC). The difference of the P_{app} values of carbamazepine dissolved from the co-crystals and from their parent physical mixtures was $2.4 \times 10^{-3} \pm 0.02 \times 10^{-3}$ cm/min in both cases (Figure 3b). Despite the ability of CBZ-VAN and CBZ-SUCC co-crystals to increase the carbamazepine permeability, no significant decrease of the NCM460 cell monolayer TEER values was registered after 60 min of their incubation in the "Millicell" systems (Figure 3c). Also the presence of NPO, as co-crystal or its physical mixture, did not induce any effect on TEER value of the monolayers (Figure 3c), while it induced significant decreases of the P_{app} value of carbamazepine ($P <$ 0.001) from $3.20 \times 10^{-3} \pm 0.05 \times 10^{-3}$ cm/min to $2.09 \times 10^{-3} \pm 0.03 \times 10^{-3}$ cm/min (MIX CBZ NPO) or $1.11 \times 10^{-3} \pm 0.02 \times 10^{-3}$ cm/min (COC CBZ NPO, Figure 3b). The overall results obtained with NCM460 cells indicate that carbamazepine appears able to slightly reduce the integrity of the cell monolayer. This effect was not influenced by the presence of succinic or vanillic acids as mixtures with CBZ, whereas their presence as co-crystals mantained the cell monolayer integrity. The same effect was registered with NPO, both as mixture and as co-crystal (Figure 3c). On the other hand, the presence of succinic and vanillic acids as mixtures with CBZ induced a decrease of its permeability across the cell monolayer, whereas their presence as co-crystals induced permeation increase. The presence of NPO, both as mixture and as co-crystal, induced a decrease of CBZ permeability across the cell monolayer (Figure 3b). Taken together, these results confirm that the effects on a biological system of a pharmaceutical co-crystal can be drastically different from those exerted by the parent physical mixture (as observed in the presence of succinic and vanillic acids), even if this is not a systematic phenomenon (as shown in the case of NPO). Therefore, we can hypothesize that the molecular aggregations of an API can be influenced by the interactions with its coformers, not only in the solid state but also in solution. Molecular aggregates resulting from dissolution, although transient, could interact with the macromolecular structures of a biological system (lipid bilayers, proteins, etc.) inducing different effects depending on the type of solid dissolved, i.e., a pure crystal, a co-crystal, or its physical mixture.

In order to verify these hypotheses, we have complemented our experimental results by performing *in silico* density functional theory (DFT) and extensive classical molecular dynamics (MD) simulations, as described in the following.

Dimer Formation in Solution: Strength and Nature of the Pair Interactions. To explore the strength and nature of the intermolecular interactions in water solution, we considered different dimers by starting from the main H-bond and π-stacking patterns discussed above (Figure 1) and exploring other possible conformations. The calculated the binding energies of the dimers examined are listed in Table 1, and their structures reported in Figure 4. These data quantify the tendency of the carbamazepine and coformers to interact once dissolved in water solution and give us a guidance to rationalize the CBZ dissolution behavior previously discussed. It is worthwhile to stress indeed that supramolecular interactions taking place in solution, and even in different solvents, can be significantly different from those observed in a crystal, where molecular packing and collective effects modify the aggregation patterns.[43] Here we recall that CBZ exists in four anhydrous polymorphic forms and a dihydrate form (DH), with CBZ(III) as the most stable anhydrous form at room temperature (aqueous solubility of CBZ(III), 0.38 mg/mL; dihydrate, 0.13

Table 1. Calculated (M06-2X/6-31G*) Binding Energies (kJ/mol) in Water Solution of the Investigated Dimers

system	dimer	binding energy (kJ/mol)
CBZ	CBZ-CBZ_H	−51.5
	CBZ-CBZ_S	−43.9
CBZ-VAN	CBZ-VAN_H	−64.0
	CBZ-VAN_S	−45.2
	CBZ-VAN_SH	−41.4
CBZ-SUC	CBZ-SUC_HA	−42.3
	CBZ-SUC_HB	−28.9
CBZ-NPO	CBZ-NPO_SH	−45.6
	CBZ-NPO_S	−49.8

mg/mL at 25 °C).[33] In an aqueous environment, the carbamazepine polymorphic forms I−III all convert to the DH form.[34]

If, on one hand, this is sufficient to explain the stabilization at lower solubility (0.18 mg/mL) displayed in Figure 2, the different curve profiles, that is, the kinetics of the CBZ DH polymorph formation, recorded for the various systems seem, instead, to be related to peculiar drug−coformer interactions, impeding/favoring the "organization" of the CBZ in the DH form. Apparently, two CBZ molecules have a considerable tendency to interact via both H-bond (−51.5 kJ/mol) and π-stacking (−43.9 kJ/mol). It is important to point out here that in the calculation of these binding energies the water is described implicitly as a polarizable continuum medium, screening the solute−solute electrostatic interactions proportionally to its polarity. Conversely, one can expect that, in solution, the dominant H-bond interactions of the carboxylic functionality will take place with water molecules. Indeed, at the same level of theory, the calculated binding energy for the coordination of two water molecules with a CBZ molecule is around 80 kJ/mol. VAN is the coformer giving the overall strongest interactions: more than 64 kJ/mol for the H-bonding and around 41−45 kJ/mol for π-stacked dimers (Table 1). Comparable values are found for the CBZ-NPO dimers, with 45.6 kJ/mol for the SH complex, characterized by both H-bond and stacking interactions (see Figure 4), and about 50 kJ/mol for another π-stacked dimer (Table 1).

The absence of aromatic rings in SUC overall weakens the interactions, with the calculated maximum value of about 42 kJ/mol. According to this static 1:1 picture, both NPO and VAN might equally compete with water and CBZ molecules in the interaction with carbamazepine and therefore alter, at a comparable extent, the dissolution profile of the drug. This seems not to be the case of the succinic acid, for which no particularly strong interactions are predicted.

MD Simulations of MIXs and COCs. Looking back at the curves in Figure 2, we can rationalize the increase in the CBZ solubility when an excess of VAN is present (i.e., in the physical mixture) on the basis of the strong CBZ−VAN interactions, possibly boosting the CBZ dissolution while competing with the CBZ−water−CBZ interactions for the DH polymorph formation. On the contrary, the effect of the other coformers and the difference between co-crystals and physical mixtures remain unclear. Although the strength of the CBZ−NPO interactions is comparable in magnitude to that of the stacked CBZ-CBZ and CBZ-VAN complexes, the NPO presence in the physical mixture produces no appreciable effects on the solubility profile of the carbamazepine, whereas its presence as co-crystal induced an immediate low solubility, similarly to
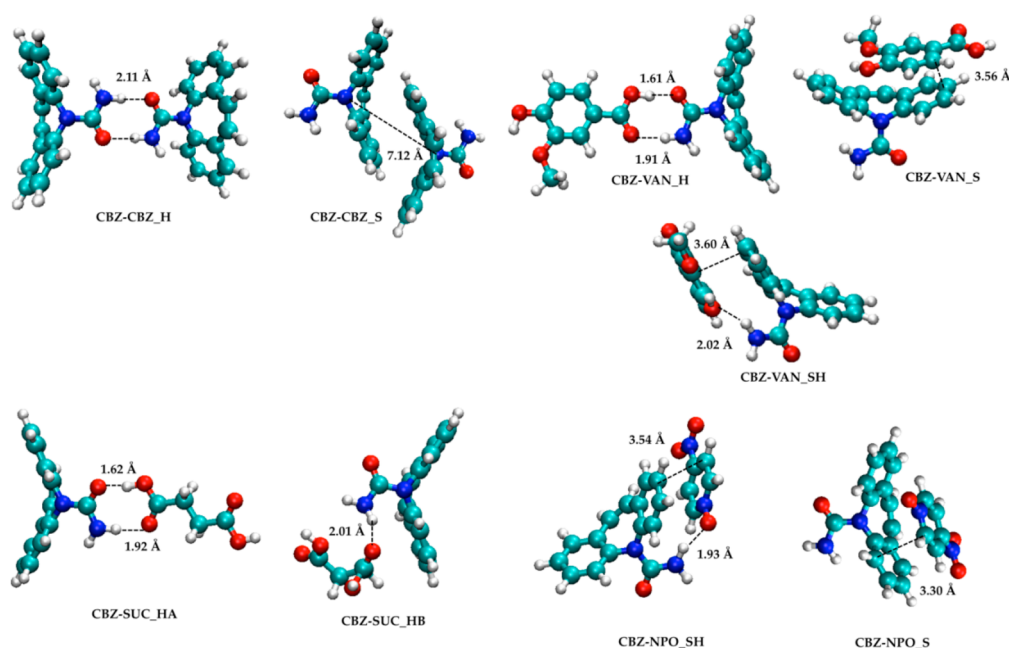
Figure 4. Optimized molecular structures of the H-bonded (H), π-stacked (S), and H-bonded and π-stacked (SH) dimers of CBZ-CBZ, CBZ-VAN, CBZ-SUC, and CBZ-NPO. Some representative interatomic distances are also reported.
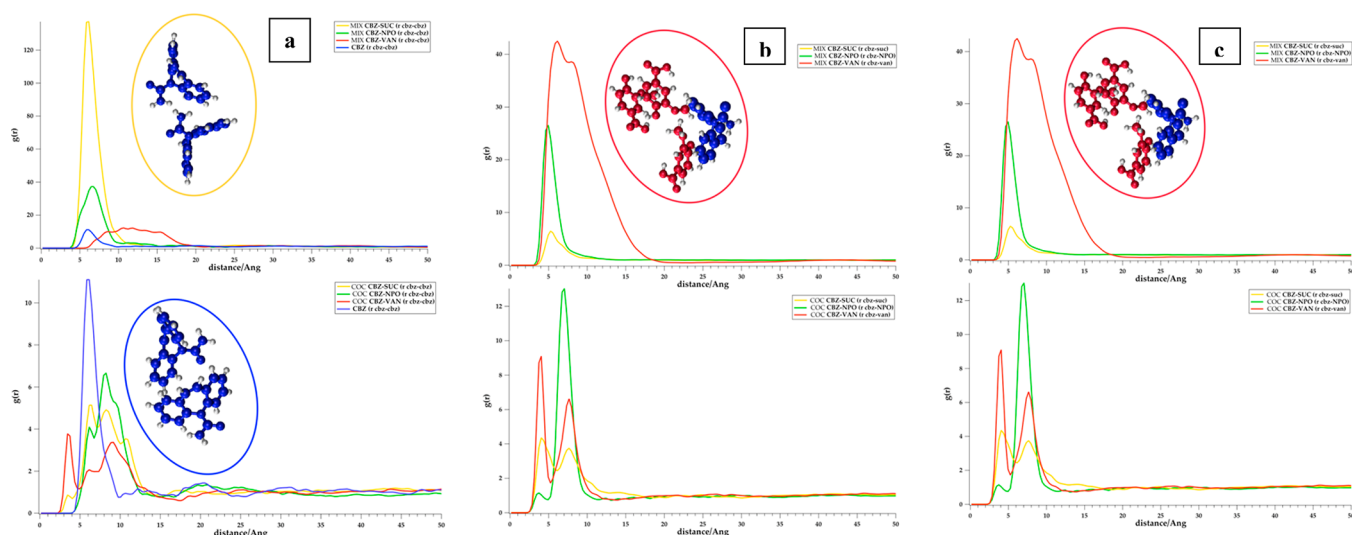
Figure 5. Atom−atom radial distribution functions, $g(r)$, of (a) the N atom of the CBZ molecules for all the simulated co-crystals (COC) and physical mixtures (MIX) as well as for the CBZ crystal (see legends and Figure S9 for further details) [two randomly extracted snapshots representative of the CBZ-CBZ dimers formed during the MIX CBZ-SUC (top plot, within the yellow circle) and CBZ (bottom plot, within the blue circle) simulations are also displayed]; (b) the N atom of the CBZ molecules in relation to a C atom of the coformers for all the simulated co-crystals (COC) and physical mixtures (MIX) (see legends and Figure S9 for further details) [a representative VAN-CBZ aggregate extracted from the MIX CBZ-VAN simulation is also displayed (top plot, within the red circle)]; (c) a C atom of the coformer molecules for all the simulated co-crystals (COC) and physical mixtures (MIX) (see legends and Figure S9 for further details) [a representative VAN-CBZ aggregate extracted from the MIX CBZ-VAN simulation is also displayed (top plot, within the red circle)].

the physical mixture and co-crystals of SUC (see Figure 2). Exploiting MD simulations we can take into account different ratios between drugs and coformers, explicit presence of water, and thermal and vibrational fluctuations. To monitor the formation of drug−drug, drug−coformer, and coformer−coformer dimers or even larger supramolecular aggregates along the MD trajectories, we will follow their average distances by calculating the pair radial distribution functions (RDFs) between two selected atoms belonging to the carbamazepine and coformer molecules (the atom selection is depicted in

Figure S9). Representative snapshots (at 0 and 40 ns) extracted from the MD trajectories of the CBZ-CBZ and CBZ-VAN, CBZ-SUC, and CBZ-NPO physical mixtures (MIXs) are also displayed in Figure 6.

The first remarkable result emerges in the top panel of Figure 5a, where the CBZ-CBZ distance is monitored. A sharp and intense peak (7.5 Å) appears in the case of the mixture of carbamazepine and succinic acid (yellow curve). Hence, the presence of an excess of SUC in solution seems to favor and promote the interaction and "dimerization" among the
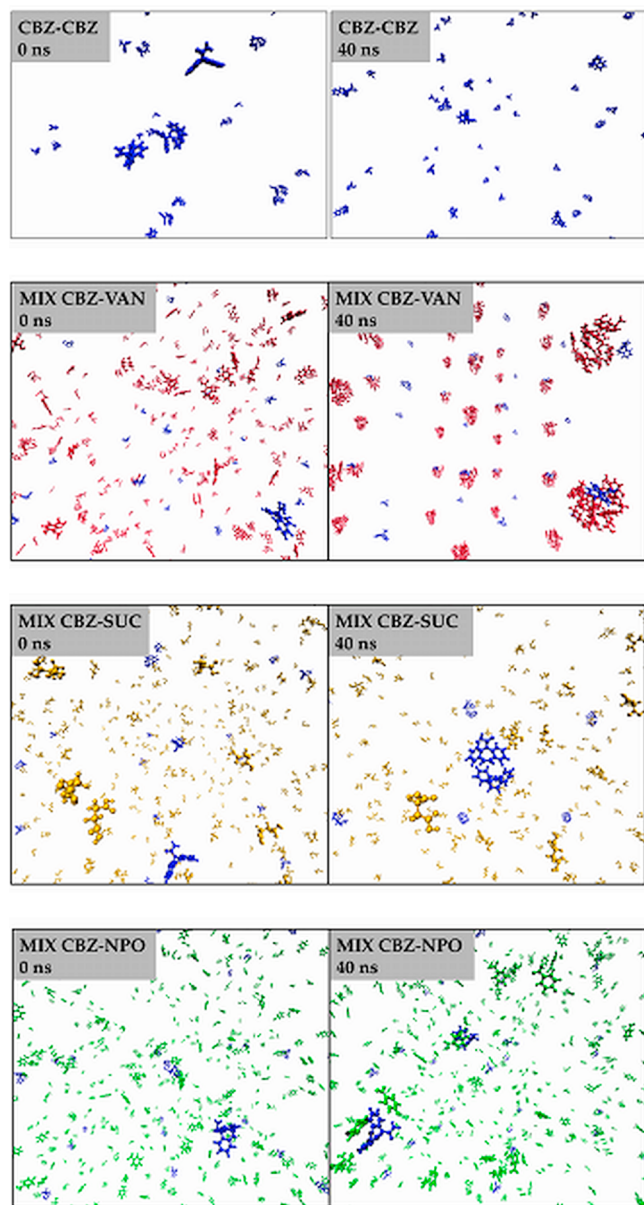
Figure 6. Snapshots extracted at 0 and 40 ns from the MD trajectories for the CBZ-CBZ and CBZ-VAN, CBZ-SUC, and CBZ-NPO mixtures. CBZ is always in blue, VAN in red, SUC in gold, and NPO in green.

carbamazepine molecules, as also apparent in the snapshot extracted from the MD trajectory after 40 ns (Figure 6). A representative dimer extracted from the MD trajectory is also reported in Figure 5a. More interestingly, this CBZ-CBZ peak is much less intense (a ratio of ca. 10:140) in the case of the simulation of CBZ alone (blue curve). A moderate and slightly broadened peak is also obtained in the case of the mixture with NPO, even if this is not appreciable in the extracted snapshots in Figure 6. The drug molecules seem, instead, to "lose" the freedom to interact with each other, and possibly organizing themselves to form the DH polymorph, when an excess of VAN is present (see the broadened red curve in the top of Figure 5a). The snapshot at 40 ns reported in Figure 6 clearly exemplifies this effect: the CBZ molecules remain, indeed, "trapped" within the aggregates (5−6 monomers) formed by the vanillic acid molecules, with the consequent inhibited

formation of the DH polymorph. Inspection of the co-crystal data (bottom panel) provides further information on the strength of the CBZ−coformer interactions, exemplified by their tendency to remain at close distances starting from the co-crystal structure. In this respect, as expected, the CBZ-VAN co-crystal shows the shorter distance peak, around 3.5 Å, closely matching the distance calculated for the CBZ-VAN_S π-stacked dimer in Figure 4.

Complementary information comes out from plots of the $g(r)$ curves in Figures 5b and 5c, where the CBZ−coformer and coformer−coformer distances are reported, respectively. In the top panel of Figure 5b, an intense peak at ca. 5.5 Å with an evident shoulder at 9 Å is obtained for the CBZ−VAN distance (red curve), indicative of strong interactions and quite structured cluster formation, as we already noticed discussing the snapshot at 40 ns for MIX CBZ-VAN in Figure 6 (see the structure of a representative aggregate shown in Figure 5b). Weaker peaks around 5 Å are also obtained for NPO and SUC. Clearly the intensity of these peaks correlates with the interaction energies calculated at the DFT level of theory and listed in Table 1: VAN > NPO > SUC.

It is interesting to compare the data in the top (physical mixture) and bottom (co-crystals) plots in Figure 5c, where the effect of the different concentrations on the coformer−coformer interactions is analyzed. In the case of the vanillic acid (red curves), the increased concentration (from 4 molecules in the co-crystal plot to 20 molecules in the physical mixture plot, see computational details above) completely changes the profile: a sharp and intense peak at about 4 Å and a second, more broadened, satellite peak at around 6−7 Å appear, again indicating the formation of supramolecular clusters, whereas no organized interaction is evident in the co-crystal plot. This concentration-dependent behavior is not apparent in the case of both NPO and SUC, where peaks of comparable intensities at about 4 and 7 Å are obtained for both the co-crystal and physical mixture simulations, even if the different peaks observed in the bottom of Figure 5a (co-crystal) between 5 and 11 Å suggest different arrangements of CBZ to interact with itself in solution allowing it to quickly reach the DH form (see Figure 2).

Summarizing, by merging the static DFT picture with the information provided by the MD simulations we have a solid ground to interpret the main features of the solubility curves reported in Figure 3: (i) the formation of VAN-VAN aggregates trapping the CBZ molecules in the CBZ-VAN mixture (top panel of Figure 5c and inset) and impeding, *de facto*, their interactions and self-organization (red curve in the top panel of Figure 5a) nicely explains the higher CBZ solubility and retardation in the formation of the DH polymorph (Figure 2); (ii) the presence of an excess of succinic acid (physical mixture CBZ-SUC), mainly interacting with water via H-bond, strongly favors the CBZ-CBZ clustering (yellow curve in the top panel of Figure 5a), providing an explanation for the low solubility recorded in the case of the physical mixtures with succinic acid with respect to the other mixtures analyzed; (iii) in all the co-crystal simulations, not unexpected behaviors were found, evidencing however a marked difference of CBZ-CBZ or CBZ-COF of COF-COF interactions between the co-crystal of vanillic acid and the other two (COC CBZ-SUC; COC CBZ-NPO), in line with the absence of appreciable change in the drug solubility observed in Figure 2 for COC CBZ-VAN. Thus, the computational analysis supports the hypothesis that the molecular aggregates of CBZ obtained by dissolution of the co-

crystals with vanillic and succinic acids are different in comparison with those obtained by the dissolution of the respective parent physical mixtures. No marked differences were, instead, predicted when NPO is involved, fully confirming the experimental findings.

CONCLUSIONS

It is known that co-crystallization can improve the solubility and permeability of APIs without changing their molecular structure, often obtaining an increase of the bioavailability of orally administered drugs.[1] In the present study it has been observed that the co-crystallization of carbamazepine with vanillic and succinic acids induces an increase of CBZ permeability across human intestinal cell monolayers. On the other hand, it has also been noticed that the effects produced by the parent physical mixtures are markedly different from those obtained by the co-crystals. According to MD simulations and DFT modeling, these differences may be attributed to different molecular aggregations formed in water by dissolving CBZ from co-crystals or from their parent physical mixtures. In agreement with what we have previously found about the different biological effects of co-crystals and parent physical mixtures of indomethacin,[6] this study remarks that pharmaceutical co-crystals can be considered not always as simply physical mixtures, but rather as new entities potentially able to produce different pharmacological effects. Our results seem therefore to confirm that new and interesting perspectives can be achieved through the application of pharmaceutical products containing co-crystals. As a consequence, appropriate investigations appear necessary in order to evaluate the potential new applications and the potential damaging effects of pharmaceutical co-crystals.

ASSOCIATED CONTENT

Ⓢ Supporting Information

The Supporting Information is available free of charge on the ACS Publications website at DOI: 10.1021/acs.molpharmaceut.7b00899.

Synthesis and characterization procedures, calculation and experimental details, geometric parameters, hydrogen bonding parameters, ORTEP views, packing diagrams, and XRD spectra (PDF)

AUTHOR INFORMATION

Corresponding Authors

*Phone: +39-0532-455144. Fax: +39-0532- 455953. E-mail: frt@unife.it.

*Phone: +39-0532-455476. Fax: +39-0532- 455953. E-mail: pvnbbr@unife.it.

*UMR SRSMC 7565 CNRS—Université de Lorraine, Boulevard des Aiguillettes, BP 70239, 54506 Vandoeuvre-lès-Nancy Cedex, France. Phone:+33-3-72745276. Fax: +33-3-72745271. E-mail: mariachiara.pastore@univ-lorraine.fr.

ORCID Ⓘ

Valeria Ferretti: 0000-0001-5515-9615

Antonio Monari: 0000-0001-9464-1463

Notes

The authors declare no competing financial interest.

ABBREVIATIONS USED

API, pharmaceutical active ingredient; COC, co-crystal; MIX, physical mixture; CBZ, carbamazepine; VAN, vanillic acid; SUC, succinic acid; NPO, 4-nitropyridine N-oxide; Pic, picric acid; 2ampyr, 2-aminopyrimidine; triaz, 2,4-diamino-6-phenyl-1,3,5-triazine; PBS, phosphate buffered saline; TEER, trans-epithelial electrical resistance

REFERENCES

(1) Dalpiaz, A.; Pavan, B.; Ferretti, V. Can Pharmaceutical Co-crystals Provide an Opportunity to Modify the Biological Properties of Drugs? *Drug Discovery Today* 2017, 22, 1134−1138.

(2) Kalepu, S.; Nekkanti, V. Insoluble Drug Delivery Strategies: Review of Recent Advances and Business Prospects. *Acta Pharm. Sin. B* 2015, 5, 442−453.

(3) Hodgson, J. ADMET-turning Chemicals into Drugs. *Nat. Biotechnol.* 2001, 19, 722−726.

(4) Bolla, G.; Nangia, A. Pharmaceutical Cocrystals: Walking the Talk. *Chem. Commun.* 2016, 52, 8342−8360.

(5) Jampílek, J.; Dohnal, J. In *Carbohydrates—Comprehensive Studies on Glycobiology and Glycotechnology*; Chang, C., Ed.; Intech Open Science: 2012; pp 81−116.

(6) Ferretti, V.; Dalpiaz, A.; Bertolasi, V.; Ferraro, L.; Beggiato, S.; Spizzo, F.; Spisni, E.; Pavan, B. Indomethacin Co-Crystals and their Parent Mixtures: does the Intestinal Barrier Recognize them Differently? *Mol. Pharmaceutics* 2015, 12, 1501−1511.

(7) Oktabec, Z.; Kos, J.; Mandelova, Z.; Havelkova, L.; Pekarek, T.; Rezacova, A.; Placek, L.; Tkadlecova, M.; Havlicek, J.; Dohnal, J.; Jampílek, J. Preparation and Properties of New Co-crystals of Ibandronate with Gluco-or Galactopyranoside Derivatives. *Molecules* 2010, 15, 8973−8987.

(8) Kos, J.; Pentakova, M.; Oktabec, Z.; Krejcik, L.; Mandelova, Z.; Harokova, P.; Hruskova, J.; Pekarek, T.; Dammer, O.; Tkadlecova, M.; Havlicek, J.; Vinsova, J.; Kral, V.; Dohnal, J.; Jampílek, J. Crystallization Products of Risedronate with Carbohydrates and their Substituted Derivatives. *Molecules* 2011, 16, 3740−3760.

(9) Dai, X.-L.; Li, S.; Chen, J. M.; Lu, T. B. Improving the Membrane Permeability of 5-Fluorouracil via Cocrystallization. *Cryst. Growth Des.* 2016, 16, 4430−4438.

(10) Jung, M. S.; Kim, J. S.; Kim, M. S.; Alhalaweh, A.; Cho, W.; Hwang, S. J.; Velaga, S. P. Bioavailability of Indomethacin-saccharin Cocrystals. *J. Pharm. Pharmacol.* 2010, 62, 1560−1568.

(11) Bethune, S. J.; Schultheiss, N.; Henck, J. O. Improving the Poor Aqueous Solubility of Nutraceutical Compound Pterostilbene through Cocrystal Formation. *Cryst. Growth Des.* 2011, 11, 2817−2823.

(12) Sarraguça, M. C.; Ribeiro, P. R.; Santos, A. O. D.; Lopes, J. A. Batch Statistical Process Monitoring Approach to a Cocrystallization Process. *J. Pharm. Sci.* 2015, 104, 4099−4108.

(13) Kuminek, G.; Cao, F.; Bahia de Oliveira da Rocha, A.; Gonçalves Cardoso, S.; Rodríguez-Hornedo, N. Cocrystals to Facilitate Delivery of Poorly Soluble Compounds Beyond-rule-of-5. *Adv. Drug Delivery Rev.* 2016, 101, 143−166.

(14) Duggirala, N. K.; Perry, M. L.; Almarsson, Ö.; Zaworotko, M. J. Pharmaceutical Cocrystals: Along the Path to Improved Medicines. *Chem. Commun.* 2016, 52, 640−655.

(15) Yan, Y.; Chen, J. M.; Lu, T. B. Synthon Polymorphs of 1:1 Co-crystal of 5-fluorouracil and 4-hydroxybenzoic Acid: their Relative Stability and Solvent Polarity Dependence of Grinding Outcomes. *CrystEngComm* 2013, 15, 6457−6460.

(16) Sanphui, P.; Devi, V. K.; Clara, D.; Malviya, N.; Ganguly, S.; Desiraju, G. R. Cocrystals of Hydrochlorothiazide: Solubility and Diffusion/Permeability Enhancements through Drug−Coformer Interactions. *Mol. Pharmaceutics* 2015, 12, 1615−1622.

(17) Gopi, S. P.; Ganguly, S.; Desiraju, G. R. A Drug-Drug Salt Hydrate of Norfloxacin and Sulfathiazole: Enhancement of in Vitro Biological Properties via Improved Physicochemical Properties. *Mol. Pharmaceutics* **2016**, *13*, 3590−3594.

(18) Brittain, H. G. Cocrystal Systems of Pharmaceutical Interest: 2010. *Cryst. Growth Des.* **2012**, *12*, 1046−1054.

(19) Brittain, H. G. Pharmaceutical Cocrystals: The Coming Wave of New Drug Substances. *J. Pharm. Sci.* **2013**, *102*, 311−317.

(20) Li, Z.; Matzger, A. J. Influence of Coformer Stoichiometric Ratio on Pharmaceutical Cocrystal Dissolution: Three Cocrystals of Carbamazepine/4-Aminobenzoic Acid. *Mol. Pharmaceutics* **2016**, *13*, 990−995.

(21) Lu, E.; Rodríguez-Hornedo, N.; Suryanarayanan, R. A Rapid Thermal Method for Cocrystal Screening. *CrystEngComm* **2008**, *10*, 665−668.

(22) Artursson, P.; Karlsson, J. Correlation Between Oral Drug Absorption in Humans and Apparent Drug Permeability Coefficients in Human Intestinal Epithelial (Caco-2) Cells. *Biochem. Biophys. Res. Commun.* **1991**, *175*, 880−885.

(23) Pal, D.; Udata, C.; Mitra, A. K. Transport of Cosalane—a Highly Lipophilic Novel Anti-HIV Agent—across Caco-2 Cell Monolayers. *J. Pharm. Sci.* **2000**, *89*, 826−833.

(24) Raje, S.; Cao, J.; Newman, A. H.; Gao, H.; Eddington, N. D. Evaluation of the Blood-brain barrier Transport, Population Pharmacokinetics, and Brain Distribution of Benztropine Analogs and Cocaine Using in vitro and in vivo Techniques. *J. Pharmacol. Exp. Ther.* **2003**, *307*, 801−808.

(25) (a) Zhao, Y.; Truhlar, D. G. The M06 Suite of Density Functionals for Main Group Thermochemistry, Thermochemical Kinetics, Noncovalent Interactions, Excited States, and Transition Elements: Two New Functionals and Systematic Testing of Four M06-class Functionals and 12 Other Functionals. *Theor. Chem. Acc.* **2008**, *120*, 215−241. (b) Pastore, M.; Mosconi, E.; De Angelis, F. Computational Investigation of Dye−iodine Interactions in Organic Dye-sensitized Solar Cells. *J. Phys. Chem. C* **2012**, *116*, 5965−5973.

(26) Cossi, M.; Rega, N.; Scalmani, G.; Barone, V. Energies, Structures, and Electronic Properties of Molecules in Solution with the C-PCM Solvation Model. *J. Comput. Chem.* **2003**, *24*, 669−681.

(27) Frisch, M. J.; Trucks, G. W.; Schlegel, H. B.; Scuseria, G. E.; Robb, M. A.; Cheeseman, J. R.; Scalmani, G.; Barone, V.; Mennucci, B.; Petersson, G. A.; Nakatsuji, H.; Caricato, M.; Li, X.; Hratchian, H. P.; Izmaylov, A. F.; Bloino, J.; Zheng, G.; Sonnenberg, J. L.; Hada, M.; Ehara, M.; Toyota, K.; Fukuda, R.; Hasegawa, J.; Ishida, M.; Nakajima, T.; Honda, Y.; Kitao, O.; Nakai, H.; Vreven, T.; Montgomery, J.; Peralta, J. E.; Ogliaro, F.; Bearpark, M.; Heyd, J. J.; Brothers, E.; Kudin, K. N.; Staroverov, V. N.; Kobayashi, R.; Normand, J.; Raghavachari, K.; Rendell, A.; Burant, J. C.; Iyengar, S. S.; Tomasi, J.; Cossi, M.; Rega, N.; Millam, N. J.; Klene, M.; Knox, J. E.; Cross, J. B.; Bakken, V.; Adamo, C.; Jaramillo, J.; Gomperts, R.; Stratmann, R. E.; Yazyev, O.; Austin, A. J.; Cammi, R.; Pomelli, C.; Ochterski, J. W.; Martin, R. L.; Morokuma, K.; Zakrzewski, V. G.; Voth, G. A.; Salvador, P.; Dannenberg, J. J.; Dapprich, S.; Daniels, A. D.; Farkas, Ö.; Foresman, J. B.; Ortiz, J. V.; Cioslowski, J.; Fox, D. J. *Gaussian09*, Revision A.1; Gaussian, Inc.: Wallingford, CT, 2009.

(28) Wang, J.; Wolf, R. M.; Caldwell, J. W.; Kollman, P. A.; Case, D. A. Development and Testing of a General Amber Force Field. *J. Comput. Chem.* **2004**, *25*, 1157−1174.

(29) Martínez, L.; Andrade, R.; Birgin, E. G.; Martínez, J. M. Packmol: A package for building initial configurations for molecular dynamics simulations. *J. Comput. Chem.* **2009**, *30*, 2157−2164.

(30) (a) Case, D. A.; Cerutti, D. S.; Cheatham, T. E., III; Darden, T. A.; Duke, R. E.; Giese, T. J.; Gohlke, H.; Goetz, A. W.; Greene, D.; Homeyer, N.; Izadi, S.; Kovalenko, A.; Lee, T. S.; LeGrand, S.; Li, P.; Lin, C.; Liu, J.; Luchko, T.; Luo, R.; Mermelstein, D.; Merz, K. M.; Monard, G.; Nguyen, H.; Omelyan, I.; Onufriev, A.; Pan, F.; Qi, R.; Roe, D. R.; Roitberg, A.; Sagui, C.; Simmerling, C. L.; Botello-Smith, W. M.; Swails, J.; Walker, R. C.; Wang, J.; Wolf, R. M.; Wu, X.; Xiao, L.; York, D. M.; Kollman, P. A. *AMBER 2016*; University of California: San Francisco, 2016. (b) Case, D. A.; Cheatham, T. E.; Darden, T.;

Gohlke, H.; Luo, R.; Merz, K. M.; Onufriev, A.; Simmerling, C.; Wang, B.; Woods, R. J. The Amber Biomolecular Simulation Programs. *J. Comput. Chem.* **2005**, *26*, 1668−1688.

(31) Humphrey, W.; Dalke, A.; Schulten, K. VMD: Visual Molecular Dynamics. *J. Mol. Graphics* **1996**, *14*, 33−38.

(32) Burnett, M. N.; Johnson, C. K. *ORTEPIII*; Report ORNL-6895; Oak Ridge National Laboratory: Oak Ridge, TN, USA, 1996.

(33) Reboul, J. P.; Cristau, B.; Soyfer, J. C. 5H-Dibenz[b,f]-azepinecarboxamide-5 (carbamazepine). *Acta Crystallogr., Sect. B: Struct. Crystallogr. Cryst. Chem.* **1981**, *37*, 1844−1848.

(34) Murphy, D.; Rodríguez-Cintrón, F.; Langevin, B.; Kelly, R. C.; Rodríguez-Hornedo, N. Solution-mediated Phase Transformation of Anhydrous to Dihydrate Carbamazepine and the Effect of Lattice Disorder. *Int. J. Pharm.* **2002**, *246*, 121−134.

(35) Tian, F.; Zeitler, J. A.; Strachan, C. J.; Saville, D. J.; Gordon, K. C.; Rades, T. Characterizing the Conversion Kinetics of Carbamaze-pine Polymorphs to the Dihydrate in Aqueous Suspension Using Raman Spectroscopy. *J. Pharm. Biomed. Anal.* **2006**, *40*, 271−280.

(36) Qiao, N.; Wang, K.; Schlindwein, W.; Davies, A.; Li, M. In Situ Monitoring of Carbamazepine-nicotinamide Cocrystal Intrinsic Dissolution Behaviour. *Eur. J. Pharm. Biopharm.* **2013**, *83*, 415−426.

(37) Yan, Y.; Chen, J. M.; Lu, T. B. Simultaneously Enhancing the Solubility and Permeability of Acyclovir by Crystal Engineering Approach. *CrystEngComm* **2013**, *15*, 6457−6460.

(38) Moyer, M. P.; Manzano, L. A.; Merriman, R. L.; Stauffer, J. S.; Tanzer, L. R. NCM460, a Normal Human Colon Mucosal Epithelial Cell Line. *In Vitro Cell. Dev. Biol.: Anim.* **1996**, *32*, 315−317.

(39) Sahi, J.; Nataraja, S. G.; Layden, T. J.; Goldstein, J. L.; Moyer, M. P.; Rao, M. C. Cl− transport in an Immortalized Human Epithelial Cell Line (NCM460) Derived from the Normal Transverse Colon. *Am. J. Physiol.* **1998**, *275*, C1048−1057.

(40) Liu, Z. H.; Shen, T. Y.; Zhang, P.; Ma, Y. L.; Moyer, M. P.; Qin, H. L. Protective Effects of Lactobacillus Plantarum against Epithelial Barrier Dysfunction of Human Colon Cell Line NCM460. *World J. Gastroenterol.* **2010**, *16*, 5759−5765.

(41) Pereira, C.; Costa, J.; Sarmento, B.; Araujo, F. Cell-based in vitro Models for Intestinal Permeability Studies. In *Concepts and Models for Drug Permeability Studies: Cell and Tissue Based in vitro Culture Model*; Sarmento, B., Ed.; Woodhead Publishing Series of Biomedicine, number 79; Elsevier: Amsterdam, 2016; pp 57−82.

(42) Ingels, F. B. M. G. P.; Deferme, S.; Destexhe, E.; Oth, M.; Van den Mooter, G.; Augustijns, P. Simulated Intestinal Fluid as Transport Medium in the Caco-2 Cell Culture Model. *Int. J. Pharm.* **2002**, *232*, 183−192.

(43) Moulton, B.; Zaworotko, M. J. From Molecules to Crystal Engineering: Supramolecular Isomerism and Polymorphism in Network Solids. *Chem. Rev.* **2001**, *101*, 1629−1658.